고성능 AC/AC 직접 전력변환을 위한 영 전압 스윗칭 싸이클로 콘버터

조 정 구 조 규 형
한 국 과 학 기 술 원 전 기 및 전 자 공 학 과

Zero Voltage Switching Cycloconverter for High Performance Direct AC/AC Power Conversion

Jung G. Cho *and* *Gyu H. Cho*
Dept. of Electrical and Electronics Engineering, KAIST

ABSTRACT

A soft switched matrix converter is proposed by adopting the zero voltage switching technique being used in some resonant pole inverters. High operating frequency with safe and efficient switching improves dynamic and spectral performances and simplifies protection logics and snubber networks. Further, it can be implemented using simple analog circuits, having similar transfer characteristics to those of the modern pulse width modulated matrix converters such as, maximum voltage transfer ratio and unity input displacement factor. Analyses, design and simulation results are presented to verify the operating principle.

I. INTRODUCTION

In recent years, nine-switch matrix converter has received considerable attention with the progress of power device technology. The fundamentals of conversion theory and PWM control strategies of the matrix converter are well established by Ziogas[1] and Venturini[2] and consequently, the maximum voltage transfer ratio was found to 0.866, for sinusoidal input and output waveforms.[2]

The matrix converter has distinctive advantages over the traditional rectifier-inverter type frequency changers, such as four quadrant operation ability and high dynamic performance. However, it has a number of problems unsolved yet such as complex protection logic and snubber networks, complex control and large input filter size due to low switching frequency. If these problems are overcome, it would be very promising alternative to rectifier-inverter type frequency changers. More recently, the research activities are oriented to find the PWM control algorithm simple enough to implement with the current microprocessors.[3,4]

On the other hand, the performance of the rectifier-inverter type frequency changers have been improved recent years by introducing the soft switching techniques[5-7], which give high frequency operation capability with current switching devices(20*KHz*). Consequently, the size of reactive components for link and filter is considerably reduced and the overall dynamic performance is also improved. Soft switching techniques for matrix converter, however, are not applied and not reported yet in the literature.

This paper proposes a new soft switched matrix converter utilizing the zero voltage switching technique similar to the resonant pole inverters.[7,8] Simply by incorporating the LC resonant and filter elements to output port of the hard switched matrix converter and connecting the neutrals of the input and output filter capacitors, the soft switched matrix converter is generated as shown in Fig. 1. Since the basic switching operation and control method are very similar to those of the resonant pole inverters,[7] the output voltage control is quite simple enough to implement with analog circuits. Safe and efficient switching operation makes high frequency operation possible without any additional snubber networks. Accordingly, the input filter size can be reduced and high dynamic performance and high spectral performance of output

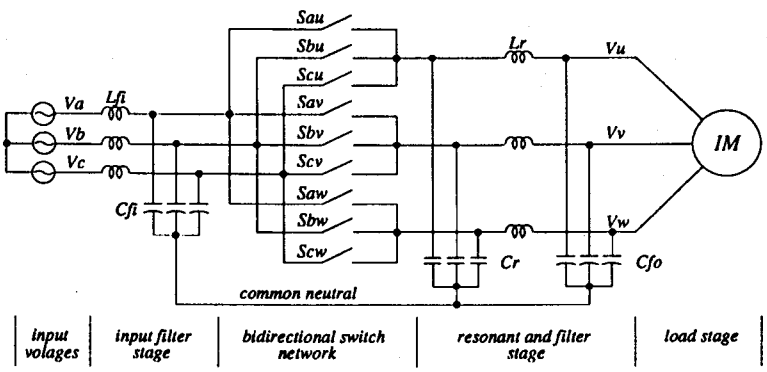

Fig. 1 Circuit topology of the proposed zero voltage switching three phase matrix converter

voltage can be obtained. The device voltage and current stresses are very low, even though the device voltage and or rms current stresses of the soft switched converters are generally much higher than those of the hard switched ones. Thus, the proposed soft switched matrix converter can overcome most of the previously mentioned problems.

Basic operation, analysis and practical implementation are presented and verified by computer simulation.

II. REVIEW OF MODERN MATRIX CONVERTER

The concept of direct frequency changers was firstly exploited by Gyugyi and then the considerable attentions have been concentrated particularly on nine-switch three-pulse matrix converter. Many researchers have been involved to develop the effective control methods and conversion theory. In consequence, the fundamentals of the conversion theory were established.[1,2] Ziogas[1] has analyzed the voltage conversion theory using the concept of rectifier-inverter to provide maximum theoretical output voltage capability.

Venturini and Alesina[2] have demonstrated an intrinsic limit of voltage transfer ratio and, independent of control algorithm, found to be 0.866 for sinusoidal input and output waveforms and the maximum voltage transfer ratio could be obtained by adding the third harmonics of the input and output frequencies to the desired output voltage as follows. For a given set of three phase input voltages

$$[V_i(t)] = \begin{bmatrix} V_i \cos(\omega_i t) \\ V_i \cos(\omega_i t - 2\pi/3) \\ V_i \cos(\omega_i t + 2\pi/3) \end{bmatrix} \quad (1)$$

The maximum output voltage amplitude can be obtained by giving the desired output voltage as

$$[V_o(t)] = [M(t)]\cdot[V_i(t)] = \begin{bmatrix} V_o \cos(\omega_o t) + \frac{V_i}{4}\cos(3\omega_i t) - \frac{V_o}{6}\cos(3\omega_o t) \\ V_o \cos(\omega_o t - \frac{2\pi}{3}) + \frac{V_i}{4}\cos(3\omega_i t) - \frac{V_o}{6}\cos(3\omega_o t) \\ V_o \cos(\omega_o t + \frac{2\pi}{3}) + \frac{V_i}{4}\cos(3\omega_i t) - \frac{V_o}{6}\cos(3\omega_o t) \end{bmatrix} \quad (2)$$

instead of giving

$$[V_o(t)] = \begin{bmatrix} V_o \cos(\omega_o t) \\ V_o \cos(\omega_o t - 2\pi/3) \\ V_o \cos(\omega_o t + 2\pi/3) \end{bmatrix} \quad (3)$$

where $M(t)$ is switching function. For $\omega_o = 1.5\omega_i$, the target output phase voltage to obtain the maximum line-to-line voltage is shown in Fig. 2 with given input voltages.

III. PRINCIPLE OF OPERATION

A. Basic Principle

The basic principle of the proposed soft switched matrix converter is phase voltage based conversion and requires the dc-link to maintain zero voltage switching operation. Thus, the Venturini's third harmonic method and Ziogas's rectifier-inverter emulation method are mixed to provide the maximum transfer ratio, 0.866 and zero voltage swithcing, simultaneously.

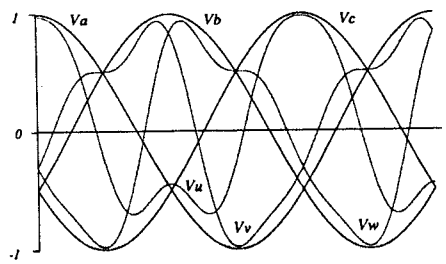

Fig. 2 Target output voltage waveforms for obtaining maximum output voltage: $V_o = 0.886V_i$ when $\omega_o = 1.5\omega_i$

To simplify the operation, one of the output phases can be separated by replacing the induction motor load with ideal current source as shown in Fig. 3 and the input filter is assumed as ideal and balanced so that the filter output voltage V^*_{abc} can be taken to be equal to the source phase voltage V_{abc}.

Three switches in Fig. 3, can be selected one at a time and rectifying operation is occurred by moderate selection of switches as shown in Fig. 4(b). Fig. 4(c) shows the fictitious dc-link which exhibits the positive and negative envelopes of the input phase voltage of Fig. 4(a) and thus, the rectifier output voltage is obtained as follows

$$V_{dc} = V_p - V_n, \quad (4)$$

which is 3 ϕ full bridge rectifier output voltage itself.

From the fictitious dc-link, the inverting operation is governed by the concept of resonant pole inverter with reference voltages given at Eq.(2) as shown in Fig. 4(c), dotted line. The inverting operation with zero voltage switching and steady state analysis are to be described at the following section.

B. Inverting Operation with Soft Switching

From the given rectifier switching pattern, the circuit of Fig. 3 can be further simplified as shown in Fig. 5 to describe the detailed switching operation and inverting action. In Fig. 5, V_p, V_n and S_p, S_n denote the positive and negative envelopes of the fictitious dc-link and switches corresponding to the rectifier switching pattern at a certain time, respectively. Since the switching frequency is generally much higher than the frequencies of input or output voltages, the V_p, V_n

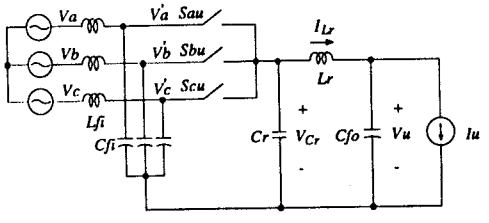

Fig. 3 Separation of a output phase

and V_U can be assumed constant over a switching period to simplify the analysis of the switching operation. The steady state inverting operation from the given fictitious dc-link, can be analyzed as follows.

One switching cycle can be divided into four modes and the associated equivalent circuits are shown in Fig. 6. Suppose that the two switches are all off and the initial resonant capacitor voltage and resonant inductor current are V_p and I_1, respectively. At time T_0, the switching cycle starts by turning on S_p with zero voltage condition.

(i) Mode 1 (T_0, T_1); S_p: *on*, S_n: *off*

As shown in Fig. 6(a), the capacitor voltage V_{C_r} is fixed by source voltage V_p. Then, the inductor current I_{L_r} is increased linearly with given initial current I_1 as

$$I_{L_r}(t) = \frac{V_p - V_u}{L_r} t + I_1. \tag{5}$$

At time T_1, the inductor current reaches its positive reference value I_2 and we obtain

$$I_2 = \frac{V_p - V_u}{L_r}(T_1 - T_2) + I_1. \tag{6}$$

(ii) Mode 2 (T_1, T_2): S_p: *off*, S_n: *off*

At time T_1, the switch S_p is turned off with zero voltage condition and L_rC_r begins to resonate with the initial conditions, I_2 and V_p, respectively. In this case, I_{L_r} and V_{C_r} become

$$I_{L_r}(t) = I_2 \cdot \cos(\omega_r t) + \frac{V_p - V_u}{Z_r} \sin(\omega_r t) \tag{7}$$

$$V_{C_r}(t) = (V_p - V_u) \cdot \cos(\omega_r t) - I_2 Z_r \cdot \sin(\omega_r t) + V_u \tag{8}$$

where, $\omega_r = 1/\sqrt{L_rC_r}$ and $Z_r = \sqrt{L_r/C_r}$. The capacitor voltage V_{C_r} resonates and reaches V_n at time T_2 when I_{L_r} reaches I_3 as

$$I_3 = \sqrt{I_2^2 + \frac{V_{dc}}{Z_r^2}(V_{dc} - 2(V_u - V_N))}. \tag{9}$$

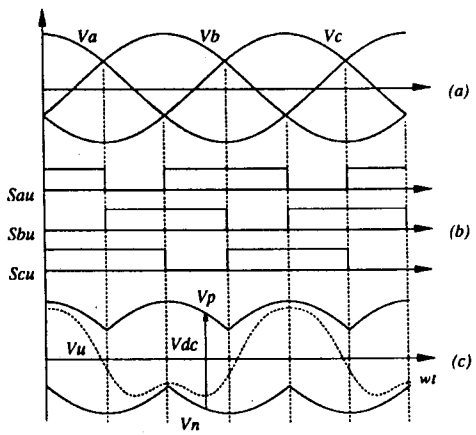

Fig. 4 Illustration of the basic operational principle: (a) three phase source voltage, (b) fictitious rectifier switching function, (c) rectifier output voltage(hidden DC link) and reference voltage of inverting operation(dotted line).

(iii) Mode 3 (T_2, T_3); S_p: *off*, S_n: *on*

In this mode, the capacitor voltage V_{C_r} is kept zero and the inductor current I_{L_r} begins to decrease linearly from its initial value I_3 to its negative reference I_4:

$$I_{L_r}(t) = -\frac{V_u - V_n}{L_r} t + I_3. \tag{10}$$

At time T_3, the inductor current reaches I_4 which is given by

$$I_4 = -\frac{V_u - V_n}{L_r}(T_3 - T_2) + I_3. \tag{11}$$

(iv) Mode 4 (T_3, T_s); S_p: *off*, S_n: *off*

At time T_3, the switch S_n is turned off with zero voltage condition and L_rC_r begins to resonate with initial conditions, I_4 and V_n, respectively:

$$I_{L_r}(t) = I_4 \cdot \cos(\omega_r t) - \frac{V_u - V_n}{Z_r} \sin(\omega_r t) \tag{12}$$

$$V_{C_r}(t) = -(V_u - V_n) \cdot \cos(\omega_r t) - I_4 Z_r \cdot \sin(\omega_r t) + V_u \tag{13}$$

When $V_{C_r}(t) = V_p$, the switch S_p is turned on with zero voltage condition and the inductor current reaches the initial

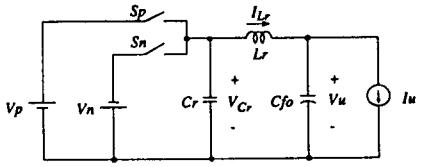

Fig. 5 Simplified circuit for illustrating inverting operation

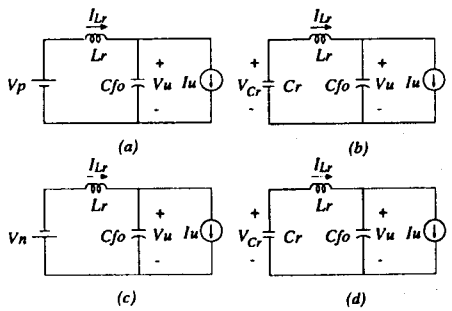

Fig. 6 Equivalent circuits for each mode: (a) Mode 1 (Sp;on, Sn;off), (b) Mode 2 (Sp;off, Sn;off), (c) Mode 3 (Sp;off, Sn;on), Mode 4 (Sp;off, Sn;off).

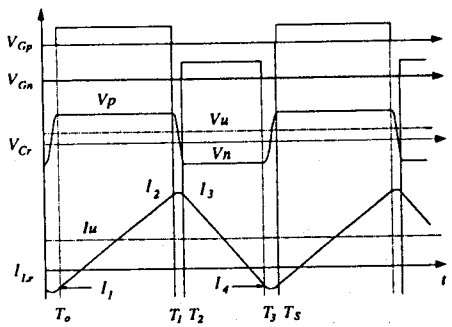

Fig. 7 Switching waveforms with gating signals.

value of mode 1, then a switching cycle is completed and we obtain

$$I_1 = \sqrt{I_4^2 + \frac{V_{dc}}{Z_r^2}(V_{dc} - 2(V_u - V_N))}. \quad (14)$$

The overall switching waveforms are shown in Fig. 7 and it is shown that the zero voltage switching occurs at every switching instant.

C. Feedback Based Output Voltage Control

The output voltage control can also be accomplished by using the control method used in the resonant pole[7]; the feedback based current mode control. The overall control block diagram and the action of inner current loop are shown in Fig. 8(a) and (b), respectively.

The inner current loop is controlled by the hysteresis current control method with variable hysteresis band. By the way, the initial current of Mode 2(I_2) and Mode 4(I_4) must be greater than a certain minimum value I_M to assure the zero voltage switching given by

$$I_M = \sqrt{\frac{2V_{dc}V_m}{Z_r}} \quad (15)$$

where $V_m = |V_u - V_{dc}/2|$. The relations of I_M and the normalized output voltage amplitude V_m/V_{dc} is also plotted with parameter Z_r in Fig. 9. To maintain the minimum initial current I_M, the hysteresis band ΔI must be varied according to reference current I_R as follows

$$\Delta I = 2(|I_R| + I_M). \quad (16)$$

The illustrative inductor current waveform when it is controlled by hysteresis current controller with variable hysteresis band is shown in Fig. 8(b).

The global voltage loop for the output voltage control can be achieved by the any kind of control algorithm, however, the conventional PI-controller is used here and current limiter is followed as shown in Fig. 8(a). By the same way, the other two output voltages can be controlled with the 120° phase difference each.

IV. PRACTICAL IMPLEMENTATION AND DESIGN CONSIDERATIONS

A. Safe Commutation

The switching devices in a matrix converter are not protected from surges existing on the ac line and the timing of the switch commutation is critical: overlap or dwell would result in a current or voltage surge across the devices during commutation. To protect these problems, the clamping circuit and complex and dissipative snubber networks have been used in the conventional matrix converter. Ref.[2] proposed the staggered commutation to simplify commutation and snubber networks, which imitates the switching operation of the dc-link inverter and thus, the bidirectional switches must be constructed with two active devices. Consequently, the overlap and dwell problems in commutation are overcome however

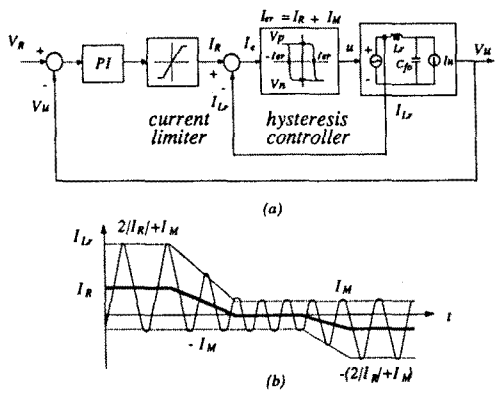

Fig. 8 Block diagram of feedback based output voltage control: (a) closed loop block diagram, (b) illustrative inductor current waveform with variable hysteresis band.

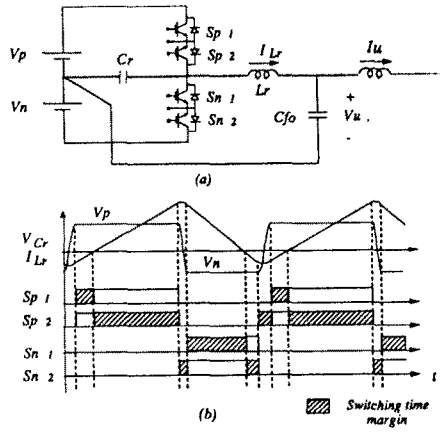

Fig. 10 Staggered commutation of the proposed matrix converter: (a) circuit for illustrating the staggered commutation, (b) switching time margins(dashed region).

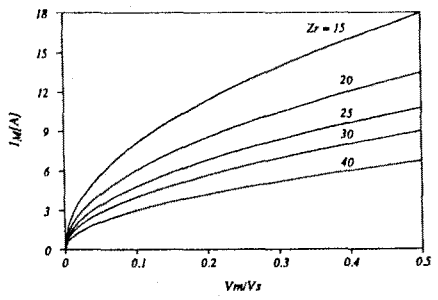

Fig. 9 Minimum initial inductor current according to the normalized output voltage for assuring zero voltage switching.

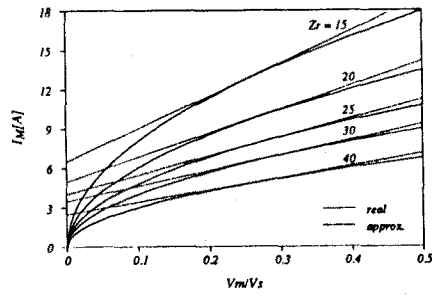

Fig. 11 Linear approximation of I_M curve for easy implementation.

the dissipative snubber networks are still required.

The proposed matrix converter can achieve the perfect staggered commutations as shown in Fig. 10. Since the resonant inductor current I_{L_r} always swings between the positive and negative value to accomplish the zero voltage switching, the outgoing switch is always active device while the incoming switch is always passive one. Further, the resonant capacitor C_r makes zero voltage condition for every switching instant and the large margin of the switching time as shown in Fig. 10(b), are always provided. Thus, the efficient and safe switching operation is always ensured without any dissipative snubber networks.

B. Simple Implementation for Minimizing Conduction Loss

The proposed matrix converter has a little bit higher conduction loss comparing with the hard switched one, since the inductor current I_{L_r} swings between the positive and negative values with a certain minimum value I_M to obtain the zero voltage switching condition. As shown in Fig. 9, the relation between the optimal value of I_M and the normalized output voltage V_m/V_{dc} is nonlinear and thus the implementation is not easy. With the given Z_r, the simple implementation can be accomplished by fixing the I_M to its maximum value. In this case, however, the conduction loss of device and reactive elements is highly increased due to wide hysteresis band. Another simple implementation can be achieved by linear approximation as shown in Fig. 11, which can be easily implemented with simple analog circuit.

V. SIMULATIONAL RESULTS

In order to verify the operational principle and predicted features, the proposed matrix converter in Fig. 1, is simulated using digital computer with simple R-L load and $220/\sqrt{3}[V]$, $60[Hz]$ source voltage. The circuit parameters used in the simulation are summerized as follows: o input filter components : $L_{fi}=10[uH]$, $C_{fi}=10[uF]$, o resonant and filter components : $C_r=0.1[uF]$, $L_r=40[uH]$, $C_{fo}=40[uF]$.

The results obtained with above parameters are shown in Fig. 12-16 for various conditions. Figs. 12-14 show the several waveforms for 30, 60 $[Hz]$ output voltage references, respectively. They show that the real output voltages follow their references with any frequency and have very high spectral performances, near sine wave. Figs. 15 and 16 show amplitude and frequency transient responses, and They show that they have very high dynamic performances.

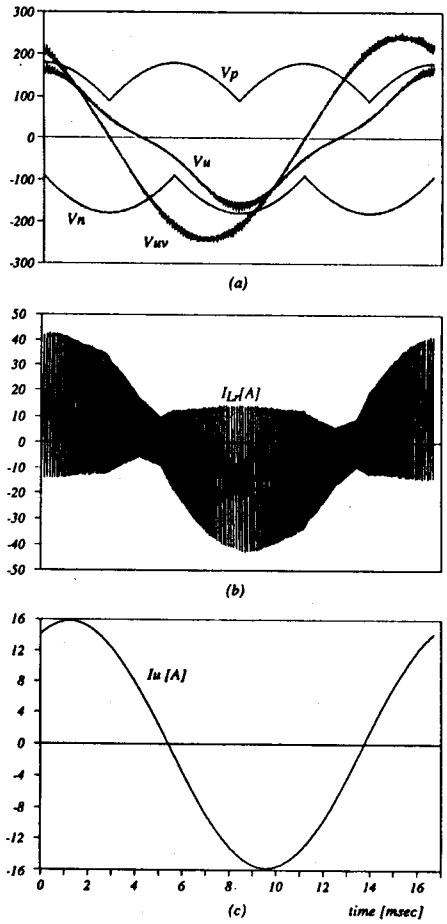

Fig. 12 Simulation results with R-L load for output voltage: 60 Hz and transfer ratio: 0.8: (a) hidden DC-link(V_p,V_n), output phase voltage(V_u), output line-to-line voltage(Vuv), (b) resonant inductor current(I_{Lr}), (c) output current(I_u).

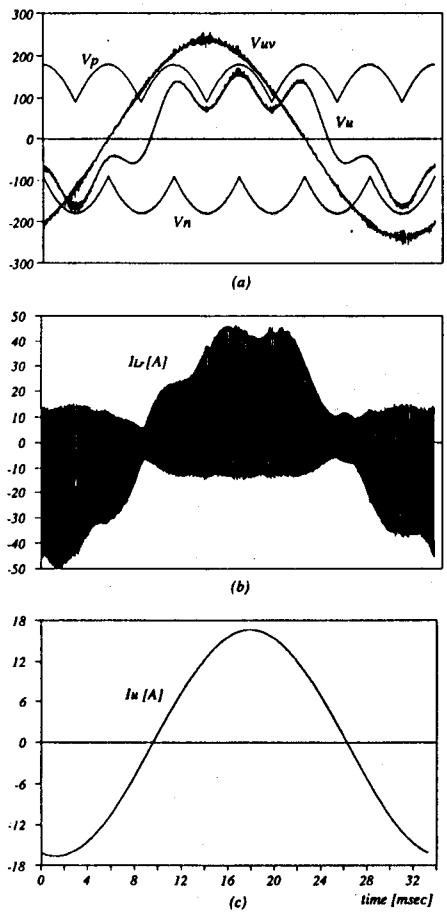

Fig. 13 Simulation results with R-L load for output voltage: 30 Hz and transfer ratio: 0.8: (a) hidden DC-link(V_p,V_n), output phase voltage(V_u), output line-to-line voltage(Vuv), (b) resonant inductor current(I_{Lr}), (c) output current(I_u).

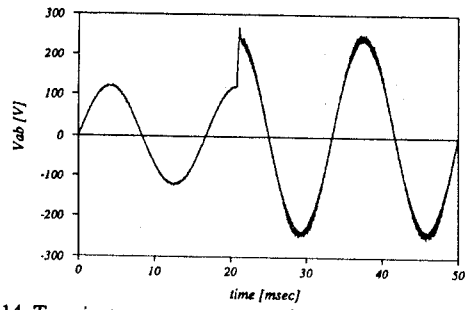

Fig. 14 Transient response: output voltage amplitude(124 V --> 249 V).

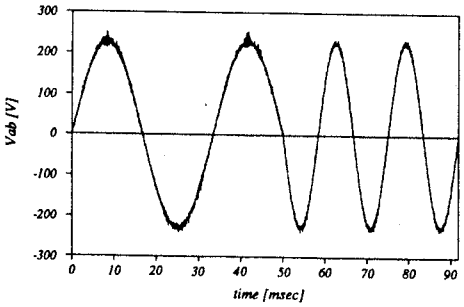

Fig. 15 Transient response: output voltage frequency(30 Hz --> 60 Hz).

VI. CONCLUSION

In this paper, the soft switched matrix converter is proposed by adopting the zero voltage switching technique used in resonant pole inverter. The operational principle and control method are also described and verified by computer simulation.

It is shown that the transfer characteristics are similar to those of the hard switched one, the maximum voltage transfer ratio and the unity input displacement factor are obtained, even though the practical voltage transfer ratio is a little bit lower than its maximum value(about 0.8). The proposed matrix converter, however, has a number of distinctive advantages over the conventional hard switched one including: low switching loss(ZVS) with low device voltage and current stresses, low EMI, no additional snubber networks, very reliable switching due to large margin of switching time, simple protection logic, very simple control, implementable with analog circuit, high dynamic performance due to high frequency operation, high spectral performance of output voltage.

Thus, the proposed matrix converter can overcome most of the problems presented in the hard switched ones and is thought to be promising converter as general frequency changer.

REFERENCES

[1] P. D. Ziogas, S. I. Khan and M. H. Rashid, "Analysis and Design of Forced Commuted Cycloconverter Structures with Improved Transfer Characteristics", IEEE Trans. on Industrial Electronics, Vol. IE-33, No. 3, August, 1986.

[2] A. Alesina and M. G. B. Venturini, "Analysis and Design of Optimum-Amplitude Nine-Switch Direct AC-AC Converters", IEEE Trans. on Power Electronics, Vol. 4, No. 1, pp. 101-112, Jan. 1989.

[3] A. Ishguro, et. al, "A New Method of PWM Control for Forced Commuted Cycloconverters using Microprocessors", IEEE IAS Rec., pp. 712-721, 1988.

[4] Y. Kim and M. Ehsani, "New Modulation Methods for Forced-Commutated Direct Frequency Changers", IEEE IAS Rec., pp. 798-809, 1989.

[5] D. M. Divan and G. Skibinski, "Zero Switching Loss Inverters for High Power Applications", IEEE IAS Rec., pp. 627-634, 1987.

[6] S. S. Park and G. H. Cho, "A Current Regulated Pulse Width Modulation Method with New Series Resonant Inverter", IEEE IAS Rec., pp. 1045-1051, 1989.

[7] J. G. Cho, D. Y. Hu and G. H. Cho, "Three Phase Sine Wave Voltage Source Inverter using the Soft Switched Resonant Poles", IEEE IECON Rec., pp. 48-53, 1989.

[8] B. S. Acharya, R. W. Gascoigne and D. M. Divan, "Active Power Filters using Resonant Pole Inverters", IEEE IAS Rec., pp. 965-973, 1989.